Research Article

For reprint orders, please contact: reprints@futuremedicine.com

Regenerative Medicine

Intestinal stem cell growth and differentiation on a tubular scaffold with evaluation in small and large animals

Aims: To investigate the growth and differentiation of intestinal stem cells on a novel tubular scaffold *in vitro* and *in vivo*. **Materials & methods:** Intestinal progenitor cells from mice or humans were cultured with myofibroblasts, macrophages and/or bacteria, and evaluated in mice via omental implantation. Mucosal regeneration was evaluated in dogs after rectal mucosectomy followed by scaffold implantation. **Results:** Intestinal progenitor cells differentiated into crypt-villi structures on the scaffold. Differentiation and scaffold coverage was enhanced by coculture with myofibroblasts, macrophages and probiotic bacteria, while the implanted scaffolds enhanced mucosal regeneration in the dog rectum. **Conclusion:** Intestinal stem cell growth and differentiation on a novel tubular scaffold is enhanced through addition of cellular and microbial components, as validated in mice and dogs.

First draft submitted: 6 April 2015; **Accepted for publication:** 4 September 2015; **Published online:** 18 September 2015

Keywords: artificial intestine • intestinal stem cells • necrotizing enterocolitis • scaffold • short bowel syndrome • tissue-engineered small intestine

Shahab A Shaffiey[‡,1], Hongpeng Jia[‡,2], Timothy Keane[3], Cait Costello[4], Deena Wasserman[1], Maria Quidgley[1], Jenna Dziki[3], Stephen Badylak[3], Chhinder P Sodhi[2], John C March[4] & David J Hackam*[,2]

[1]Division of Pediatric Surgery, Children's Hospital of Pittsburgh, 4401 Penn Avenue, Pittsburgh, PA 15217, USA

[2]Division of Pediatric Surgery, Department of Surgery, Johns Hopkins University, 600 N Wolfe Street, Baltimore, MD 21287, USA

[3]McGowan Institute for Regenerative Medicine, 450 Technology Drive Suite 300, Pittsburgh, PA 15219, USA

[4]Department of Biological & Environmental Engineering, Cornell University, Ithaca, NY 14850, USA

*Author for correspondence:
Tel.: +1 410 955 2717
Fax: +1 410 502 5314
Dhackam1@jhmi.edu

[‡]Authors contributed equally

Significant challenges exist in the development of an engineered small intestine [1–4]. These include coordinating the differentiation of various epithelial cell types that must line its surface, and the need to create a structure that has an adequate absorptive surface area [5]. Previous investigators have demonstrated the successful ability to grow intestinal progenitor cells into structures that bear similarities to the intestinal mucosa using flat scaffolds or Matrigel [1,2,6–8], suggesting the possibility that the development of a scaffold with an adequate surface area for absorption may provide additional benefit. We have developed a serial mold fabrication technique to create a 3D tubular scaffold that matches the intricate topography of the small intestine, and which has significant absorptive capacity *in vitro* [9], and have now tested the ability of this tubular scaffold to support the growth of intestinal progenitor cells isolated from mouse and human intestine. We now demonstrate that this novel *in vivo* bioreactor system can form an intact epithelial lining *in vitro* and *in vivo* that bears remarkable similarities to the native intestine. In order to further understand the steps required for optimization of the growth and differentiation of intestinal stem cells on this novel scaffold, we now test the hypothesis that the addition of various cellular components of the intestinal stem cell niche, namely macrophages and myofibroblasts, will enhance the growth and differentiation of intestinal progenitor cells upon it. Finally, we evaluate the ability of this 3D scaffold to support the growth of intestinal progenitor cells in both a murine model and a dog model. Taken together, the current findings provide evidence that a novel tubular scaffold with topologic properties that mimic the native small intestine can be optimized to support the growth and differentiation of intestinal progenitor cells when important cellular components that are

Future Medicine part of fsg

normally present in the intestinal stem cell niche are incorporated.

Materials & methods

Reagents, antibodies & animals

Lactobacillus rhamnosus was from ATCC (VA, USA; Strain:GG, ATCC#53103). *E. coli* (strain DH5a) was obtained from ATCC and was heat-inactivated at 68°C for 45 min as described [10]. The sources of the antibodies used in this study include: Invitrogen: chromogranin A, F4/80, α-smooth muscle actin, desmin, green fluorescent protein; Abcam: Ki-67, CD146, anti-Mac; Santa Cruz: lysozyme, Muc-II, proliferating cell nuclear antigen (PCNA), sucrose-isomaltase; Dako: von Willebrand Factor; Thermo Scientific: MPO; Sigma: DHE; Millipore: Anti-NG2; Roche: TUNEL kit. The epithelial marker E-cadherin (Invitrogen) was used as a reliable surrogate marker for enterocytes and has shown to be required for intestinal morphogenesis [11].

All mouse experiments performed at the University of Pittsburgh were approved by the University of Pittsburgh via Protocol #12070649 and Protocol #12040382. All mouse experiments performed at Johns Hopkins University were approved via Protocol #MO14M362. All dog studies were performed at the University of Pittsburgh via Protocol #13011355.

C57BL-6, NOD/SCID γ-chain-deficient mice, Lgr5-EGFP-IRES-creERT2, Gt(ROSA)26Sortm4(ACTB-tdTomato,-EGFP)-Luo reporter (mT/mG) mice were from Jackson Research Laboratory. Generation of Lgr5 lineage tracing reporter mice ($Lgr5^{Gt(ROSA)26Sortm4(ACTB-tdTomato,-EGFP)}$) was reported previously [12].

Primary intestinal crypt cultures (enteroids) were isolated and maintained in culture on Matrigel according to the methods of Sato *et al.* Following isolation, crypts were counted and added to Matrigel at 500 crypts/50 µl. Intestinal subepithelial myofibroblasts (ISMF) were isolated according to the technique of Lahar *et al.* [8]. Bone marrow macrophages were isolated from the femur and tibia of 14-day-old C57Bl/6 mice, cultured them in 15-cm dishes in RPMI 1640 supplemented with 10% heat-inactivated fetal bovine serum, 100 U/ml penicillin, 100 µg/ml streptomycin, 2 mM L-glutamine, 10 mM Hepes (all Gibco, Invitrogen) and 15% L-929 cell-conditioned medium (LCM) containing M-CSF for 8 days, then induced their differentiation toward an intestinal M2 phenotype by treating for 24 h with IL-4 (20 ng/ml, Peprotech) and IL-10 (10 ng/ml, R&D Systems). Flow cytometry was then performed to assure the intestinal (M2) phenotype using markers for CD206 and CD163 [13]. Cocultured enteroids with niche components performed on three separate experiments with at least ten different enteroids evaluated per experimental group.

Enteroid & niche component seeding on a polylactic-glycolic acid scaffold

Polylactic-glycolic acid (PLGA)-rich synthetic scaffolds were prepared according to our recently described study [9,14], sterilized with 70% ethanol for 24 h, then coated with Matrigel (BD Biosciences, CA, USA), diluted 1 to 10 in crypt cell media, followed by polymerization at 37°C for 45 min. Polymer design was aided first by statistical software (Stat-Ease Inc., MN, USA), which allowed for comparisons of different formulations *in silico*, and gave us a basis for the rational design and selection of the materials. In keeping with the architecture of the native mouse intestine, the height from the base to the villus tip was 500 microns with a thickness of 100 microns at the base. To select pore size, we measured the overall porosity of the scaffolds using an ethanol displacement method. To evaluate the effects of prolonged culture in a fluidic environment, the scaffolds were placed in media for 4 weeks to further evaluate porosity and evaluation of surface architecture using scanning electron microscopy. Intestinal crypt suspensions were then seeded onto the 3D scaffolds for 3 h at 37°C. Unattached crypts were then removed by washing, and samples were incubated with crypt culture growth media containing added growth factors (500 ng/ml Rspondin, 200 ng/ml WNT3a, 200 ng/ml Noggin and 50 ng/ml EGF, all from Invitrogen). Crypts were then cultured for 7 days on the scaffolds and assessed by upright confocal microscopy. For coculturing, the enteroids with niche components (n = 6/group), 10^2 cfu/ml live bacteria or 10^5 cfu/ml for heat-killed bacteria and 10^4/ml for myofibroblasts and M2 macrophages added in the culture 24 h after initiation of the enteroid culture on the apical side of the scaffold. Microbial cultures were stopped following 3 days of coculture to prevent bacterial overgrowth, whereas myofibroblasts and macrophages were cocultured for 5 days prior to being stopped for immunohistochemistry.

Implantation of enteroid-seeded tubularized PLGA scaffold into the omentum of mice

PLGA scaffolds on which enteroids had been seeded for 5 days were tubularized, then implanted into the omentum of immune-deficient NOD/SCID mice under isofluorane anesthesia through a mid-line laparotomy. The omentum was delivered and used to wrap the enteroid-loaded tubularized 3D scaffold which was then secured using a 5–0 monofilament suture placed around the omentum and scaffold itself. The omentum was then replaced within the abdomen and the incision was closed in layers with 4–0 vicryl sutures,

and the implanted scaffold with the attached cells was incubated in the host animal for 14, 28 or 35 days.

Growth of enteroids from human intestine

All human tissues were obtained with approval from the University of Pittsburgh Institutional Review Board and in accordance with the University of Pittsburgh anatomical tissue procurement guidelines. Intestinal samples and stool were obtained from human neonates undergoing resection for necrotizing enterocolitis (NEC) – a severe disorder that causes the destruction of the intestine in premature infants. Control intestinal tissue was obtained from infants undergoing surgery at the time of stoma closure as previously described [15]. Intestinal stem cells were then harvested and grown in Matrigel or on the scaffold in the same manner as the mouse cells.

PCR from human enteroids

Human enteroids from normal and diseased intestine were isolated and cultured in Matrigel (BD Biosciences, CA, USA) on 24-well plate for 3–6 days followed by addition of 0.5 ml Trizol reagent to each well to isolate total RNA according to manufacture's protocol. PCR was performed using the following primers: GAPDH, human, 5′-TCTCCTCTGACTTCAACAGCGACA-3′ (forward) and 5′-CCCTGTTGCTGTAGCCAAATTCGT-3′ (reverse); PCNA, human, 5′GAAGCACCA AACCAGGAGAA-3′ (forward), 5′-TCTCG GCATATACGTGCAAA-3′ (reverse); LGR5, human, 5′-ACCTGAAAGCCCTTCATTCA-3′ (forward), 5′-TGCTATGGTCC ACACTCCAA-3′ (reverse); lysozyme, human, 5′CCTGCAGTGCTTTGCTGCAAGAT A-3′ (forward), 5′-TCTCCATGCCACCCATGCTCTAAT-3′ (reverse); muc2, human, 5′-AGGTGCTGATCAAGACCGTGCATA-3′ (forward), 5′-ATGTCCACCACGTAGT TGATGCCA-3′ (reverse); chromogranin A, human, 5′-GAGGAGGGCAGCGCAAAC CG-3′ (forward), 5′-GGTGTCTCAGCCCCGCCGTA-3′ (reverse).

Implantation of tubularized PLGA scaffold into the intestine of dogs after mucosectomy

In order to assess the ability of the scaffold to support intestinal mucosal growth in a large animal model as a potential precursor to future use in humans, tubularized 3D scaffolds without seeding of enteroids were implanted into mongrel dogs (weight: 18–25 kg). The mucosa of the rectum and distal sigmoid colon was first removed using a transanal approach. This provided a platform for the implantation of the tubularized scaffold, and also provided access for repeated evaluation of the implanted scaffold using colonoscopy. Under general anesthesia, each dog was placed in the supine position and after aseptic preparation of the anus and rectum, a mucosectomy was performed using blunt and sharp dissection for a distance of 4 cm using electrocautery to achieve hemostasis. In control animals (n = 2), mucosectomy was performed without implantation of the scaffold. In the experimental group (n = 2), a 4-cm length of 3D tubularized scaffold was implanted into the mucosal defect using fine vicryl sutures. Dogs were then closely monitored for weight loss, bloody stools and rectal bleeding and underwent colonoscopy at 2, 4, 6 and 8 weeks postoperatively with imaging, biopsy and visual evaluation of the rectal mucosa, from the distal anus to proximal to the most proximal suture line. At the time of necropsy, the entire distal colon was resected *en bloc* including the anus, the rectum along with the entire length of the mucosectomy defect marked by proximal and distal nonabsorbable sutures. The tissue was then serially sectioned to encompass the mucosa proximal and distal to the mucosectomy site, with careful attention to maintaining proper circumferential and axial orientation. These steps significantly minimized any potential effect that the sampling error could cause.

Statistical analysis

Data for quantification were obtained by counting of positively stained cells identified by Metamorph software (Molecular Devices Corp) using imaging algorithms and computer learning to identify positive cells. Manual confirmation of positive staining was confirmed prior to analysis, and quantification was expressed as a percentage of positive cells compared with all nucleated cells by investigators blinded to the study group. All experiments were repeated at least in triplicate with more than 100 cells/high power field. For determination of the volume and surface area of the enteroids and villi, Z-stacks of each image were obtained via confocal microscopy, and analyzed using ImageJ using the 3D object counter plugin. Color thresholds were then set for measurement of each cell based upon total cellular fluorescence before the analysis and the volume and surface area were determined using an average of the number of colors incorporated into the immunostaining. For enteroids cultured on scaffold, the volume and surface area were also determined by the number of villi appearing in each field of view; five fields were counted in each group. For *in vivo* studies, omental implantation occurred in ten mice/groups per time point. Dog mucosectomy occurred with two dogs per group. Statistical analysis was performed using Stata 13.0 software. Statistical analysis included mean and standard deviation, using a two-tailed unpaired stu-

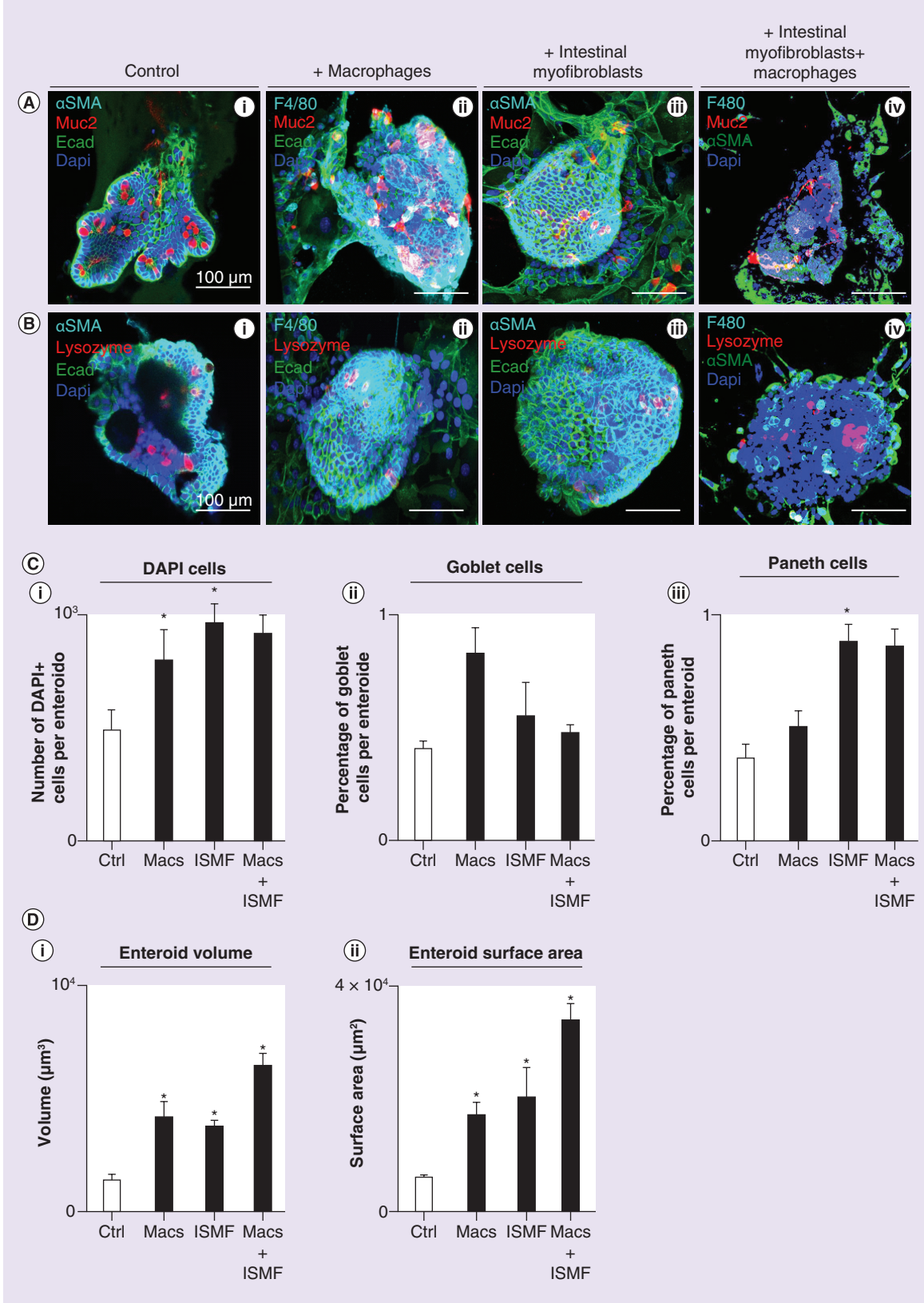

Figure 1. The coculture of mouse-derived enteroids with intestinal myofibroblasts and M2 macrophages enhances their growth and differentiation in matrigel. (A) Representative confocal images of control intestinal enteroids **(Ai & Bi)** derived from mouse ileum stained for the goblet cell marker muc–2, the enterocyte marker E-cadherin (E-cad), the paneth cell marker lysozyme and the nuclear marker DAPI. (Continued on facing page).

Figure 1. The coculture of mouse-derived enteroids with intestinal myofibroblasts and M2 macrophages enhances their growth and differentiation in matrigel (cont.). Slides were also stained for the fibroblast marker smooth muscle actin (SMA) and the macrophage marker F480. Enteroids were cultured along with macrophages **(Aii & Bii)**, intestinal subepithelial myofibroblasts **(Aiii & Biii)** and both intestinal myofibroblast and macrophages **(Aiv & Biv)**. **(C)** Quantification of the total number of cells **(i)**, and the percentage of goblet cells **(ii)** or paneth cells **(iii)**. **(Di–ii)** Quantification of volume **(i)** and surface area **(ii)** of the enteroids within the indicated groups. *Denotes significant difference between control and experimental group ($p < 0.05$); representative of three separate experiments with at least five enteroids/group. Data show all individual data points with average. Size bar = 100 μm.

dent's t-test for evaluation of two groups, ANOVA for greater than two groups. Statistical significance was defined as $p < 0.05$.

Results

Effect of the addition of cellular & bacterial components on the growth & differentiation of enteroids

We first sought to define the contribution of stem cell niche components on the growth and differentiation of enteroids, both *in vitro* and *in vivo*. As shown in Figure 1, under control conditions, intestinal crypts grew and developed into highly organized structures containing cells that expressed markers of enterocytes (E-cadherin), goblet cells (Muc2) and paneth cells (lysozyme). Interestingly, adding the stem cell niche components macrophages or intestinal myofibroblasts [8,16,17] to the crypt cultures significantly altered the general appearance of the cultures, which significantly increased in size (volume and surface area) (Figure 1Aii–iv, Bii–iv, Ci & Di), yet which were not found to act synergistically (Figure 1Aiv, Biv, Ci–iii & Di–ii). Given that intestinal crypts grow and differentiate within an environment that is rich in microbes, we next assessed the effects of clinically relevant bacterial cultures on crypt growth and differentiation. As shown in Figure 2, there was no effect on the rate of enterocyte proliferation – as measured by the expression of Ki-67 – after the addition of live or heat-killed *E. coli* or after the addition of stool obtained from an infant with NEC (Figure 2Ai–iv & Bi). By contrast, the addition of pure cultures of the probiotic bacteria *L. rhamnosus* caused a striking increase in enteroid proliferation (Figure 2Aiv & Bi). The addition of either live *E. coli* (Figure 2Avii & xii) or heat-killed *E. coli* (Figure 2Aviii & Axiii) or the addition of stool from an infant with NEC (Figure 2Ax & Axv) had subtle effects on enteroid differentiation (Figure 2Bii & Biii). These effects were characterized by a reduction in goblet cells for *E. coli* and a significant increase in goblet cells in the presence of stool from patients with NEC. Strikingly, the addition of *L. rhamnosus* significantly increased the degree of paneth cell differentiation (Figure 2Axiv & Biii). Based upon the above studies, we next sought to evaluate whether intestinal stem cells isolated from human tissue could grow and differentiate into enteroids, and to assess the expression of clinically relevant genes that a differentiated intestine would be expected to express. To do so, we obtained intestinal resection samples from infants either under control conditions (Figure 3A), or as part of the surgical treatment of NEC (Figure 3C), and assessed for their ability to grow and differentiate on Matrigel. Samples from five individual patients were analyzed. As shown in Figure 3, enteroids that were harvested from control human tissue were found to differentiate into goblet cells (Figure 3Aii), paneth cells (Figure 3Aiii) and enteroendocrine (Figure 3Aiv) cells, which was confirmed via PCR for cell-specific markers, including the proliferation gene PCNA, the intestinal stem cell gene LGR5 [18], the paneth cell gene lysozyme [19,20], the goblet cell gene MUC2 [21] and the enteroendocrine gene chromogranin A [22] (Figure 3B). Importantly, the enteroids that were grown from tissue obtained from infants undergoing surgery for NEC displayed the development of enteroids that were smaller and more spherical, but were capable of differentiation into all relevant intestinal cell-type lineages (Figure 3C), and to express relevant intestinal-specific genes (Figure 3D). Taken together, these findings illustrate that mouse and human enteroids can grow and differentiate *in vitro*, and lay the groundwork for cultures on a clinically relevant biological scaffold.

Growth & differentiation of mouse-derived intestinal progenitor cells on a novel 3D scaffold *in vitro*

We have now developed a novel scaffold that bears the 3D shape and surface area that is similar to the native small intestine including the presence of villi [9,14]. In order to extend the above findings to a physiologically relevant *in vivo* model, we next sought to determine whether this novel scaffold could support the growth of mouse-derived intestinal progenitor cells, and if so, to determine the effects of niche components or bacterial cultures on intestinal growth and differentiation. As shown in Figure 4A–C, after 7 days of culture, intestinal crypt cultures (enteroids) were observed to cover the entire synthetic villus from the base to the tip as revealed by scanning electron microscopy (Figure 4Ai). The intestinal progenitor cells were observed not only to cover the villi but to also differentiate into goblet cells (Figure 4Aii) and paneth cells (Figure 4Aiii). For contextual purposes, a schematic of the surface of the scaffold

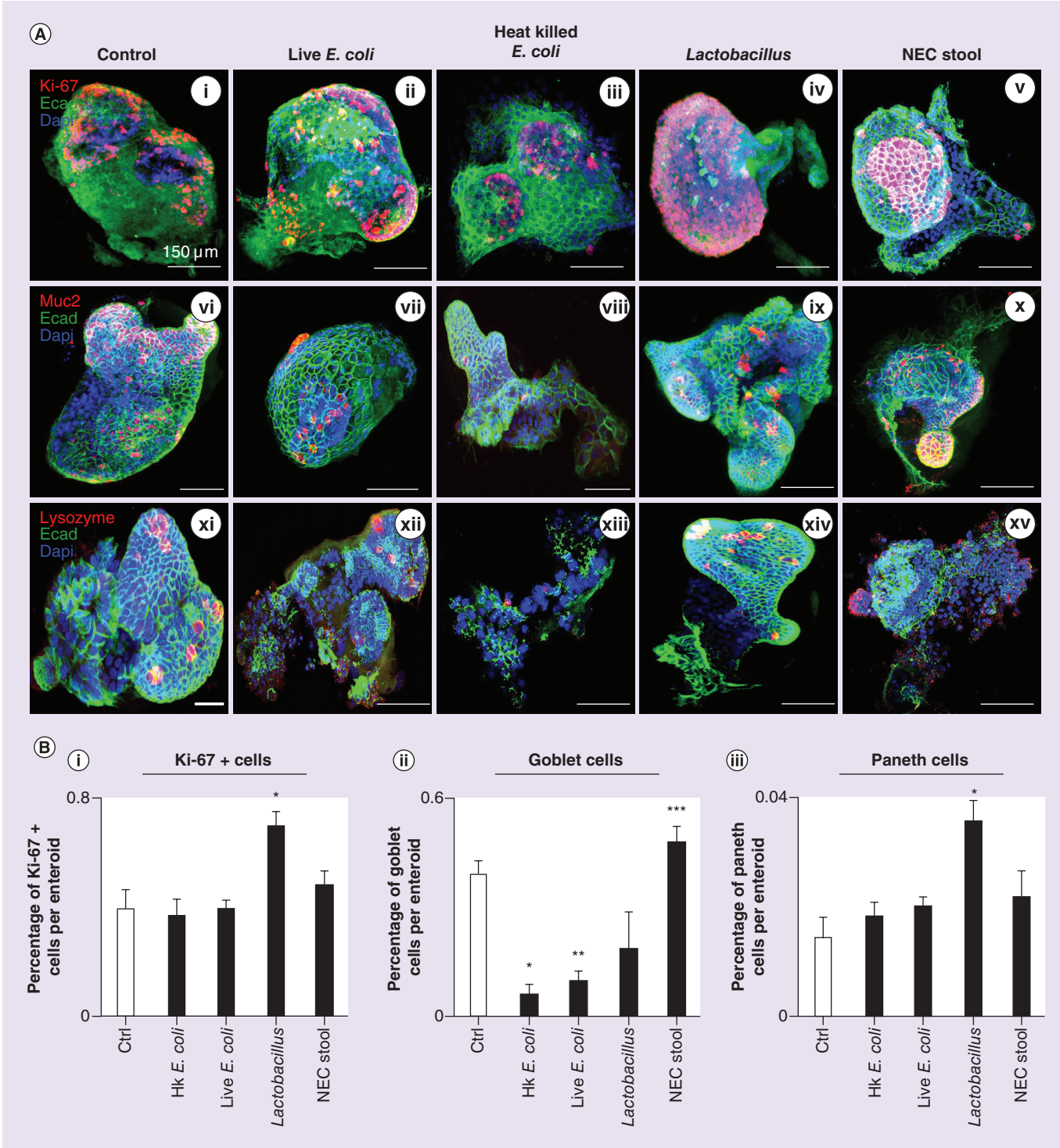

Figure 2. The effects of the addition of *E. coli*, the probiotic bacterium Lactobacillus, or stool from an infant with necrotizing enterocolitis on the growth and differentiation of enteroid cultures in matrigel. **(A)** Representative confocal images of enteroids derived from mouse intestine that were cultured for 4 days under control conditions **(Ai, vi, xi)** or with the addition of live *E. coli* **(Aii, vii, xii)**, heat-killed *E. coli* **(Aiii, viii, xiii)**, *Lactobacillus* **(Aiv, ix, xiv)** or stool from an infant with necrotizing enterocolitis **(Av, x, xv)** after 3 days of culture. As shown, slides were stained for the proliferation marker Ki67 **(Ai–v)**, the goblet cell marker Muc2 **(Avi–x)** or the paneth cell marker lysozyme **(Axi–xv)**. **(B)** Quantification of Ki-67+ve cells **(i)**, goblet cells **(ii)** and paneth cells **(iii)** in indicated groups. *Denotes significant difference between the control and experimental group ($p < 0.05$). Graphs representative of three separate experiments with at least five enteroids per group. Data mean + SEM. Scale bars as listed on imaging.

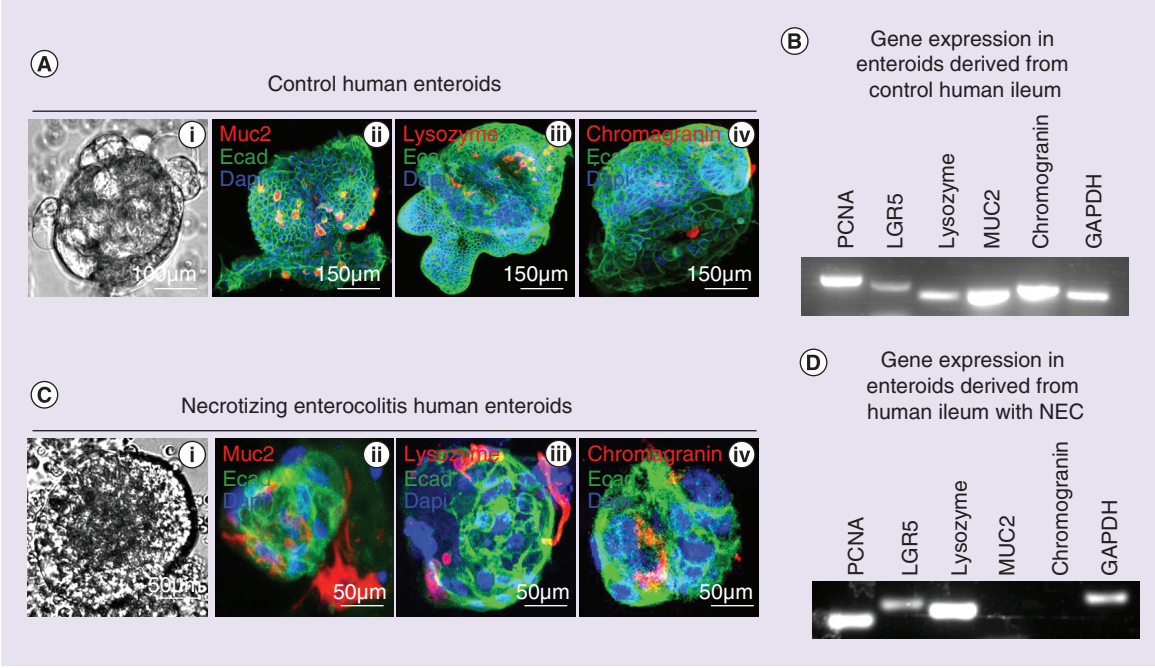

Figure 3. Growth and differentiation enteroids derived from normal and diseased human intestine. (Ai & Ci) Representative micrographs of enteroid isolated from healthy **(Ai)** neonatal small intestine at the time of ostomy closure and from the intestine removed from an infant with necrotizing enterocolitis (NEC) **(Ci)**. **(Aii–iv, Cii–iv)** Representative confocal micrographs of enteroids stained for muc2 **(Aii & Cii)**, lysozyme **(Aiii & Ciii)** and chromogranin A **(Aiv, Civ)** under the indicated conditions. Representative of over 50 similar enteroids from three independent patient samples per group. **(B & D)** rt-PCR performed for expression of the proliferation marker (PCNA), intestinal stem cells (LGR5), goblet cells(muc–2), paneth cells (lysozyme), enteroendocrine cells (chromogranin A) and housekeeping gene (GAPDH) in tissue obtained from control patients **(B)** or patients with NEC **(D)**.

on which the intestinal cells are growing is shown, in which the dimensions are indicated (Figure 4Aiv). It is noteworthy that the addition of either intestinal myofibroblasts (Figure 4Bii) or macrophages (Figure 4Biii), or the combination of the two (Figure 4Biv) increased the growth of enteroids on the scaffolds, as revealed by whole mount confocal microscopy. The volume and surface area of cell covered villi is shown in Figure 4D, revealing that the presence of macrophages and myofibroblasts increase the degree of coverage by epithelial cells, as compared with villi in which macrophages and myofibroblasts were not added. Importantly, the tubularized scaffold was also able to support the growth of enteroids in the presence of bacterial cultures, including live *E. coli, L. rhamnosus* and cultures obtained from infant stool (Figure 4C). Taken together, these findings raise the possibility that these scaffolds may be clinically relevant in the development of an artificial intestine.

Evaluation of the ability of a novel tubularized bioscaffold to support the growth of intestinal progenitor cells *in vivo*

Having shown that the novel bioscaffold that bears a similarity to the configuration of the native intestine can support the growth of enteroids *in vitro*, we next sought to evaluate its ability to support growth and differentiation when tubularized and implanted *in vivo*. To do so, we seeded the tubularized scaffold with enteroids obtained from mouse ileum and allowed them to incubate for 5 days, then implanted the tubularized seeded scaffold into the omentum of mice. As shown in Figure 5A, a sagittal view obtained after 4 weeks of implantation shows the underlying tubularized structure is largely intact, and shows evidence of the presence of structures that loosely resemble villi. Furthermore, a top-down view of one such villi (from different mice) reveals a cellular monolayer that surrounds the villus structure of the scaffold (Figure 5Aiii–iv). Similar structures were obtained when tubularized scaffolds were implanted with crypts from human infants (Figure 5Av). Next, we sought to confirm that the tissue growth that was observed around the villi was indeed from donor derived origin and not host derived. To do so, we isolated intestinal crypts from mice that express green fluorescence protein on the rapidly cycling LGR5 intestinal stem cell locus ($Lgr5^{Gt(ROSA)26Sortm4(ACTB-tdTomato,-EGFP)}$) in order to identify in the recipient mice the origin of the stem cells. As shown in Figure 5B, GFP-positive

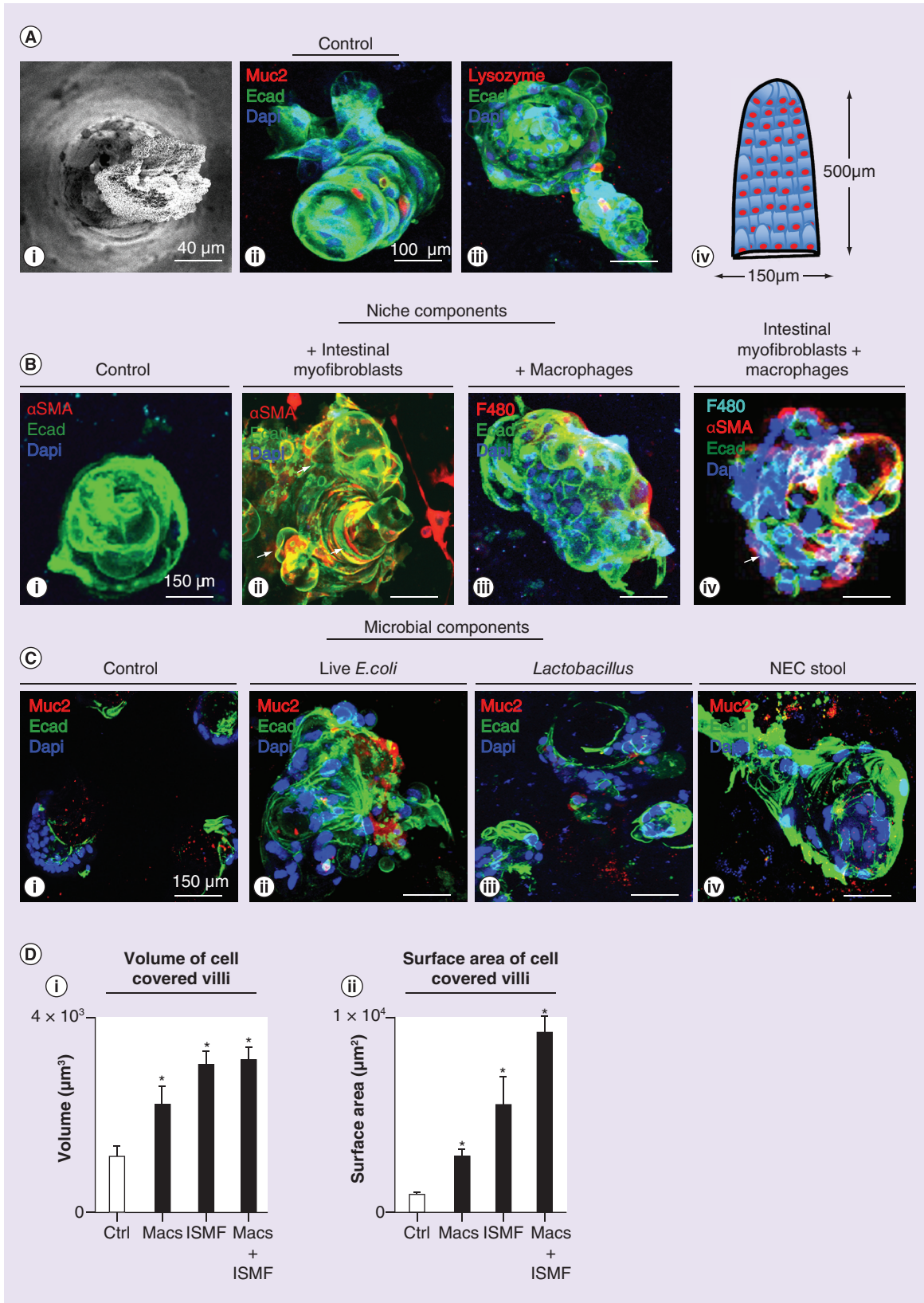
A
Control
Muc2
Ecad
Dapi
Lysozyme
Ecad
Dapi
40 µm
100 µm
500µm
150µm
Niche components
B
Control
+ Intestinal myofibroblasts
+ Macrophages
Intestinal myofibroblasts + macrophages
αSMA
Ecad
Dapi
F480
αSMA
Ecad
Dapi
150 µm
Microbial components
C
Control
Live E.coli
Lactobacillus
NEC stool
Muc2
Ecad
Dapi
150 µm
D
Volume of cell covered villi
Surface area of cell covered villi
Volume (µm³)
Surface area (µm²)
4 × 10³
1 × 10⁴
0
Ctrl
Macs
ISMF
Macs + ISMF

Figure 4. Growth of intestinal progenitor cells on a novel 3D scaffold can be enhanced with the addition of niche and microbial components (see facing page). (A) Representative scanning electron microscopic **(i)** or confocal images **(ii–iii)** or a single synthetic villus upon which murine intestinal progenitor cells had been seeded, allowed to grow for 5 days in culture, then stained for the indicated cellular markers. For contextual purposes, a schematic of the surface of the scaffold on which the intestinal cells are growing is shown, in which the dimensions are indicated **(iv)**. **(B)** Representative scanning confocal micrograph of individual synthetic villi on which murine intestinal progenitor cells had been seeded under control conditions **(i)** or along with intestinal myofibroblasts **(ii)** or macrophages **(iii)** or both intestinal myofibroblasts and macrophages **(iv)**; slides were stained with smooth muscle actin **(i–ii)** or macrophages **(iii)** or both **(iv)** as shown. Arrows reveal macrophages or myofibroblasts in the respective panels. **(C)** Representative confocal images of synthetic villi upon which enteroids were seeded for 4 days under control conditions **(i)** or with live *E. coli***(Cii)**, *Lactobacillus rhamnosus***(Ciii)**, and stool from an infant with necrotizing enterocolitis **(Civ)**. Representative of over 50 synthetic villi from three independent experiments. **(Di–ii)** Quantification of volume **(i)** and surface area **(ii)** of the villi within the indicated groups. *Denotes significant difference between control and experimental group ($p < 0.05$); representative of three separate experiments with at least five villi per group.

E-cadherin-positive cells were obtained within the scaffold, indicating that cells were identified within the recipient mice that were donor derived, and that could be differentiated into an epithelial lineage. Importantly, the scaffold was capable of supporting viable, proliferating cells within the omentum of mice, as demonstrated by the finding of relatively few apoptotic cells (Figure 5Ci–ii, arrows) and a high number of proliferating cells (Figure 5Ciii–iv, arrows) within the newly formed intestinal epithelium. Taken together, these findings support the ability of the novel 3D PLGA scaffold to foster epithelial growth from intestinal enteroids using an *in vivo* omental implantation model in mice.

Effect of the novel tubularized bioscaffold on the induction of blood vessels & inflammatory cells in underlying matrix in mice

We next sought to further characterize the biologic properties of the scaffold, and in particular, to determine the degree to which implantation of the scaffold influenced angiogenesis and the influx of inflammatory cells within the underlying matrix. As shown in Figure 6, implantation of the tubularized scaffold which contained enteroids resulted in the influx of blood vessels into the scaffold, as detected by immunostaining for Von Willebrand Factor (vWF) that was seen both 14 (Figure 6Aii) and 28 days (Figure 6Aiii). The enteroids themselves had some effect on the presence of the blood vessels, as these were not seen to the same degree in mice in whom implantation of scaffold alone was performed (Figure 6Ai). The effect of the scaffold on angiogenesis was confirmed by the detection of CD146/NG2-positive pericyte progenitor cells [23,24], which were detected in the underlying matrix of mice in which the scaffold containing enteroids had been implanted for either 14 (Figure 6Bii) or 28 days (Figure 6Biii), and to a lower extent in mice in which the scaffold had been implanted without enteroids (Figure 6Bi), consistent with the staining for the endothelial cells themselves (Figure 6Ai–iii). The presence of enteroids at 14 or 28 days resulted in a significant increase in the degree of immunostaining for vWF, when quantified using ImageJ (normalized pixels/high power field: empty scaffold: $5 \times 10^3 \pm 1 \times 10^3$, scaffold + enteroids 14 days: $4 \times 10^4 \pm 2 \times 10^3$, scaffold + enteroids 28 days: $4 \times 10^4 \pm 2 \times 10^3$, $p < 0.05$ by ANOVA). The implantation of the scaffold did result in the influx of macrophages, as revealed by immunostaining for F4/80 (Figure 6Ci–iii), and neutrophils (Figure 6Di–iii), as revealed by immunostaining for myeloperoxidase, which were seen in mice implanted with empty scaffold as well as scaffold containing the enteroids at both 14 and 28 days. It is noteworthy that the combination of inflammatory cells resulted in the generation of free oxygen radicals within the underlying matrix that was seen at 28 days in mice in which empty scaffold had been implanted (Figure 6Ei), and also in mice in which scaffold containing enteroids had been implanted for 14 days (Figure 6Eii), which became somewhat less prominent at 28 days (Figure 6Eiii & Supplementary Figure 1). Taken together, these findings indicate that the novel bioscaffold can induce the growth of blood vessels as well as inflammatory cells in the subscaffold matrix in mice.

A tubularized PLGA-based bioscaffold can support intestinal mucosal growth in a canine model

In the final series of studies, we sought to evaluate whether a novel PLGA-enriched scaffold could support mucosal growth *in vivo*. To do so, we removed the mucosa from the rectum and distal colon of four dogs over a length of 4 cm using a transanal approach, which provided a platform for the placement of a PLGA-rich scaffold in two dogs, which was sewn into the site of the mucosectomy. In order to evaluate the effects of the tubularized scaffold on the growth of native intestinal epithelium, no intestinal stem cells were seeded on the matrix. In control animals, mucosectomy alone was performed. As shown in Figure 7Ai, histologic evaluation confirmed that the mucosectomy removed the entire mucosa and submucosa. Colonoscopic evaluation revealed that in dogs subjected to mucosectomy alone, there was persistent inflammation, tissue friability and

ulceration at 2 and 8 weeks from surgery from the location of the proximal sutures distally (Figure 7Bi–ii). By contrast, in dogs who underwent mucosectomy followed by placement of the tubularized PLGA scaffold, the tissue friability that was seen at 4 weeks had largely resolved by 8 weeks and complete mucosal coverage was observed (Figure 7B iii–iv). Arrows are included to show the location of the distal sutures on the colonoscopic image to reveal the site of the injury in Figure 7Biii. Additional evidence for the ability of the scaffold to support intestinal mucosal growth *in vivo* was provided histologically, which shows that in the absence of the scaffold, a fibrous

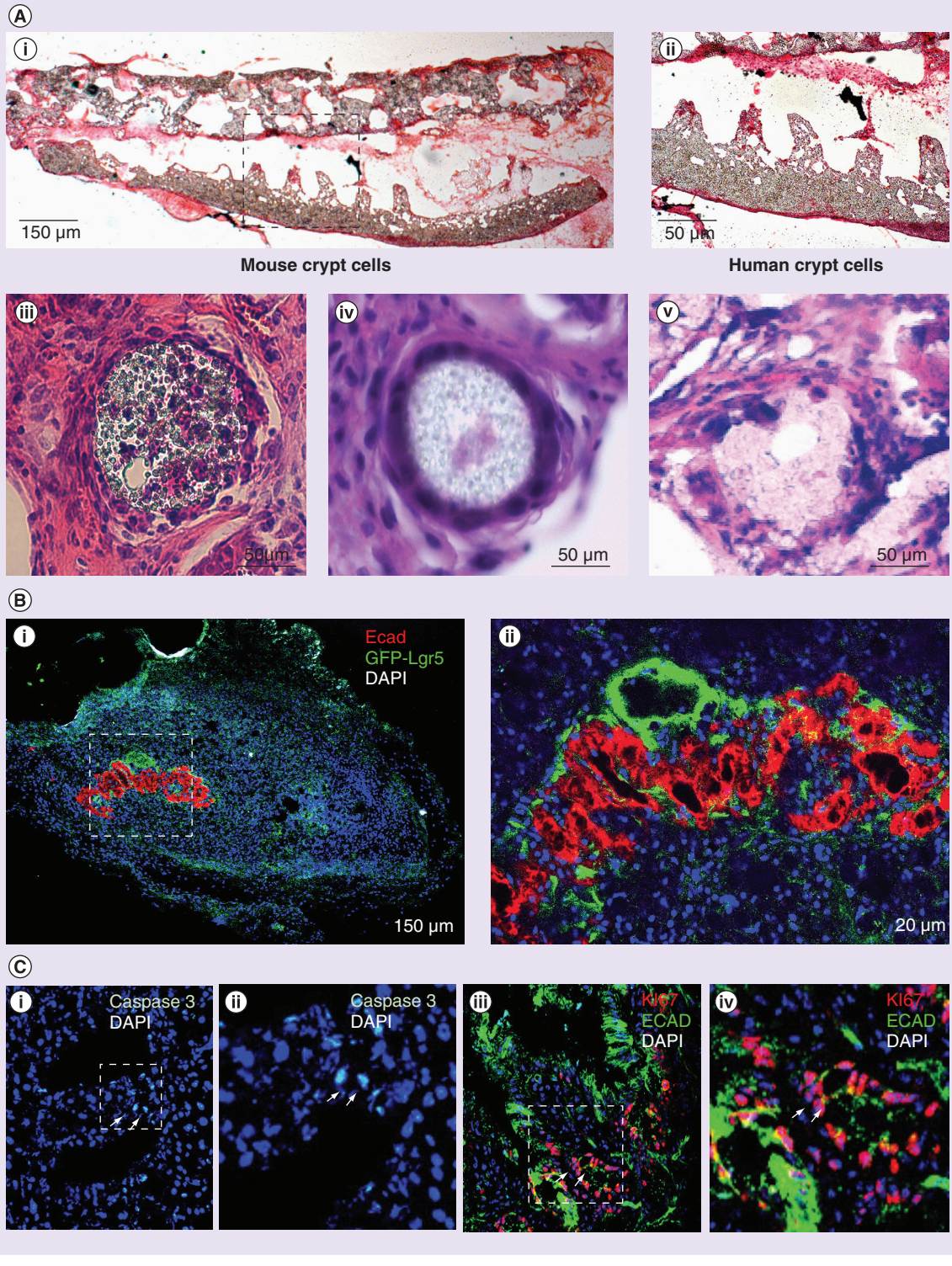

Figure 5. Implantation of a novel intestinal scaffold into mouse omentum maintains cell growth which is donor derived (see facing page). (A) Representative H&E micrographs of the omentum from a NOD/SCID mouse 28 days after implantation of synthetic scaffold that had been seeded with mouse-derived progenitor cells showing intact villous structure **(i)**; higher magnification of the demarcated area is shown **(Aii)**. **(Aiii–iv)** Top-down view of representative villi that had been seeded with intestinal progenitor cells from two separate mice **(iii-iv)**. **(Av)** Top-down view of scaffold from a NOD/SCID mouse that had been seeded with progenitor cells from human intestine. **(B)** Representative confocal micrograph of the omentum obtained from NOD/SCID mouse that had been seeded with enteroids derived from Lgr5–GFP mice stained for GFP and enterocyte marker Ecad **(Bi)**; shown is an image at higher magnification from the demarcated area **(Bii)**. Representative of three separate experiments. **(Ci–ii)** Expression of apoptotic cells (cleaved caspase three positive, arrows; panel **(ii)** represents inset in panel **(i)** at higher magnification) and **(iii–iv)**: proliferating cells (ki67 positive, arrows, panel **(iv)** represents inset in panel **(iii)** at higher magnification) of the cells growing on the scaffold under conditions shown in Panel A. Representative of three separate experiments.

layer of scar tissue replaces the mucosa, and an intact epithelium is not seen (Figure 7Ci–iv). In contrast, histologic evaluation of the distal colon of dogs subjected to insertion of the tubularized PLGA-scaffold revealed the development of a normal mucosal layer, which resembled the native overlying epithelium (Figure 7Cv–viii), which was only seen at the edges in the mucosectomy alone controls. The degradation of the scaffold in this model compared with the readily visible scaffold in the murine omental implantation model is due to frozen sectioning instead of paraffin sectioning, but based upon the colonoscopic imaging, appears to be replaced with normal colonic mucosa at approximately 3–4 weeks. Importantly, in dogs who underwent implantation of the scaffold, the colonic mucosa is rich in Alcian-blue-positive cells (Figure 8Aiii–iv) that were not seen after mucosectomy alone (Figure 8Aii), confirming the ability of the scaffold to support the growth and differentiation of native intestinal mucosa into goblet cells (Figure 8A). Moreover, in agreement with the findings observed in mice (Figure 6), the implantation of the scaffold in dogs resulted in an influx of macrophages that were seen at 4 weeks (Figure 8Biii), and yet were significantly less prominent after 8 weeks (Figure 8Biv) to levels that were similar to that observed in the normal colon (Figure 8Bi), and which were significantly lower when compared with dogs that had undergone mucosectomy alone (Figure 8Bii). Quantification of these findings is provided in Supplementary Figure 1. Taken together, these findings illustrate that the scaffold can support growth and differentiation in the native intestinal environment.

Discussion

In the current study, we report that intestinal crypts can grow and differentiate on a novel scaffold which bears striking similarities to the native small intestine. These studies advance our understanding of the development of a replacement intestine in three distinct ways. First, we now show that the growth and differentiation of mouse-derived intestinal crypt cultures (enteroids) can be optimized through the simple addition of components of the native intestine, including macrophages, intestinal myofibroblasts and certain microbes (Figures 1 & 2). Second, the growth of intestinal crypt cultures along the synthetic tubularized 3D villi is an advance over prior studies in which intestinal crypts are grown in Matrigel or flat scaffolds (Figures 4–5), and reveal that the tubularized scaffold induces the growth of blood vessels and that the degree of inflammation is tempered by the presence of the enteroids themselves (Figure 6). Finally, we show that this novel tubularized bioscaffold can support the growth of native mucosa within an anatomically appropriate site, in other words, the distal colon, raising the possibility that this scaffold can support the ability of the host to restore mucosal continuity in the face of a large surface loss (Figures 7–8). We note that the dogs stooled normally without diarrhea, suggestive of intact fluid absorption. While we acknowledge that it is known that enteroids can be grown from human tissue (e.g., Grant *et al.* [25]), ours is the first report to our knowledge of the ability to successfully grow enteroids from diseased intestine (others have shown the ability to grow enteroids at the time of stoma closure, for instance). Moreover, the added novelty of this paper lies in the demonstration of the effects of niche components on the growth and differentiation of enteroids both *in vitro* and *in vivo*, and on the role of a novel scaffold to support neointestinal growth. Taken together, these findings advance our current knowledge regarding the optimal properties required for intestinal progenitor cell growth, and raise the possibility that a synthetic intestine that is seeded with intestinal progenitor cells may be developed.

The current work extends our understanding of this current-tubularized 3D PLGA-based scaffold, and raises the possibility that it may be used as the backbone of a replacement small intestine, in particular given the enhanced growth of the intestinal crypts that was observed in the presence of additional cellular and microbial elements. Our study is the first to show the effects of using an architecturally relevant scaffold using primary intestinal progenitor cells both *in vitro* and *in vivo,* and to demonstrate that individual crypt stem cells can be transferred from one mouse and induced

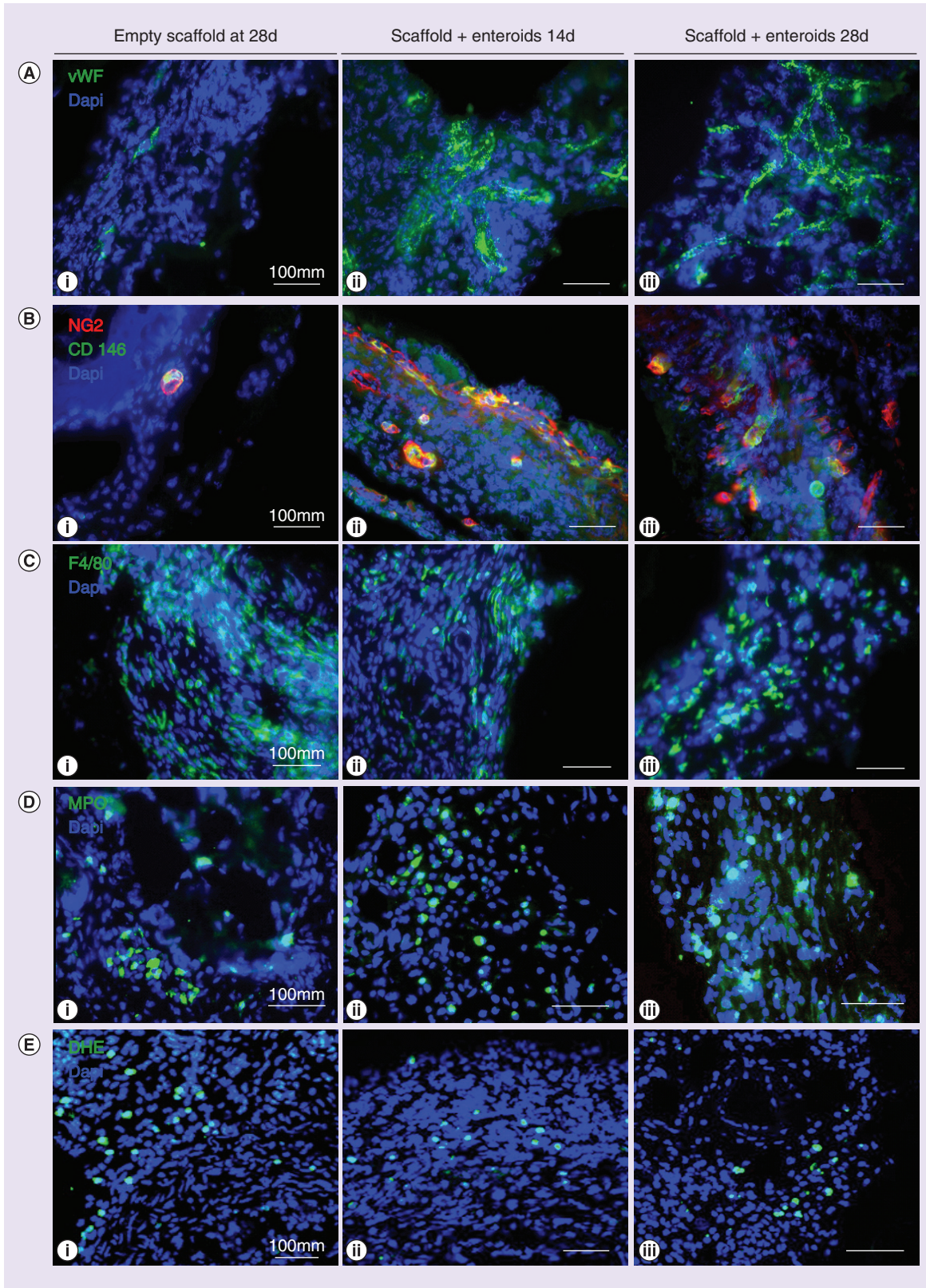

to form an epithelial monolayer on a scaffold in a different mouse. Prior research from our group has shown the importance of maintaining a 3D structure to allow for appropriate absorption, differentiation and topographical bacterial interactions compared with 2D scaffolds *in vitro* [9,14,26]. While the mechanisms by which

Figure 6. Characterization of the 3D scaffold following murine implantation (see facing page). **(A)** Evaluation of angiogenesis staining for vascular marker Von Willibrand Factor in an empty scaffold following 28 days implantation **(Ai)** and the scaffold with enteroids at 14 **(Aii)** and 28 days **(Aiii)** following implantation. **(B)** Newly formed blood vessels were evaluated using the perivascular stem cell marker NG2 colocalized with blood vessel marker CD146 in the groups noted above. **(C & D)** Evaluation of the inflammatory response of the 3D scaffold for macrophages (F4/80) and neutrophils (MPO) in the groups noted. **(E)** DHE staining performed for evaluation of reactive oxygen species in the groups noted. Representative of three separate experiments.

these niche components enhance enteroid growth are not immediately clear, there are several potential clues into their mechanisms of action. For instance, secreted products of intestinal myofibroblasts may activate Wnt and Notch pathways that can regulate cell proliferation and differentiation, respectively, and which also may play a direct role in enterocyte migration, which is important in coverage of the bioscaffold [27]. Macrophages may also release growth factors and other cytokines that can enhance migration and proliferation of adjacent epithelial cells, in part via Wnt signaling [28], and these were certainly detected in the underlying matrix in the mouse and dog models. Furthermore, the addition of bacteria can lead to activation of bacterial recognition receptors including TLR2 and 4, which could alter stem cell recruitment and survival [29]. Our prior research supports this theory. We have shown that activation of TLR4 leads intestinal stem cell loss via effects on wnt/β-catenin signaling through the downstream receptor MyD88 [12,30,31], while developmental activation of TLR4 is required for normal intestinal differentiation, through effects on TRIF [32]. Additional studies are required to discern the precise contributions of TLR activation in response to whole bacteria on intestinal stem cell growth, differentiation and development. While we choose not to specifically characterize the microbial diversity of NEC stool in this study, our group was previously shown an increase in total bacteria with no distinction in bacterial communities from matched controls but did show a decreased diversity of *Enterobacteriaceae* in NEC stool [33]. Moreover, the effects of these components on the absorption across the engineered mucosal barrier remain to be assessed directly.

We readily acknowledge that the addition of myofibroblasts and macrophages to the apical surface of epithelial cells on the scaffold may raise concerns regarding physiological relevance, as unlike microbes, these cells exert their effects largely at the basilar surface. However, for the purpose of this study, our principle goal was to determine the role – if any – of myofibroblasts and macrophages on the growth and differentiation of intestinal stem cells on a novel scaffold, and we were therefore as interested in the potential paracrine effects of these cells as in any potential direct cell–cell effects. To this end, the application of macrophages and myofibroblasts to the apical surfaced provides a ready model to assess the effects of macrophages and myofibroblasts on the growth and differentiation of intestinal stem cells in which paracrine effects could be experimentally explored. We are encouraged not only by the observation of these effects as illustrated in the manuscript but also by several studies indicating that myeloid cells can exert processes that extend up toward the apical surface, lending additional physiological relevance to the current findings, as others have reported [34,35].

A potentially clinically relevant observation from the current findings is the determination that a tubularized PLGA-rich scaffold could be used to bridge a large mucosal defect – in this case on which was surgically created – when placed within the anatomically appropriate location within the rectum. While the area subjected to mucosectomy alone had some spontaneous healing at the very edges, this was extremely negligible and significantly less than that observed in the presence of the scaffold.

The findings that the mucosa regenerated in a histologically normal manner could be interpreted to reveal that this scaffold could also be used to support mucosal growth in the setting of loss of large sections of mucosa. Such scenarios could include the transanal removal of large sessile polyps. By enhancing the ability of the body to regenerate the mucosa using this scaffold using a simple anastomotic technique, patients may benefit from enhanced mucosal regeneration and potential avoid the need for a stoma. Further experiments are required in order to determine the potential limits of mucosal resection that can be reversed with the use of an implanted scaffold.

Conclusion

We now show the beneficial effects of adding appropriate cellular and microbial components on the growth and development of intestinal stem cells on a novel scaffold system, highlight the ability to grow intestinal stem cells from one mice within the omentum of a second mouse on a biologically relevant scaffold, identify the immunological and vascular consequences of scaffold implantation and reveal the benefit of this scaffold as a mucosal replacement mechanism in a dog model of mucosectomy. These findings offer a foundation for additional studies in testing the absorptive and functional capacities of this intestinal cell lined structure.

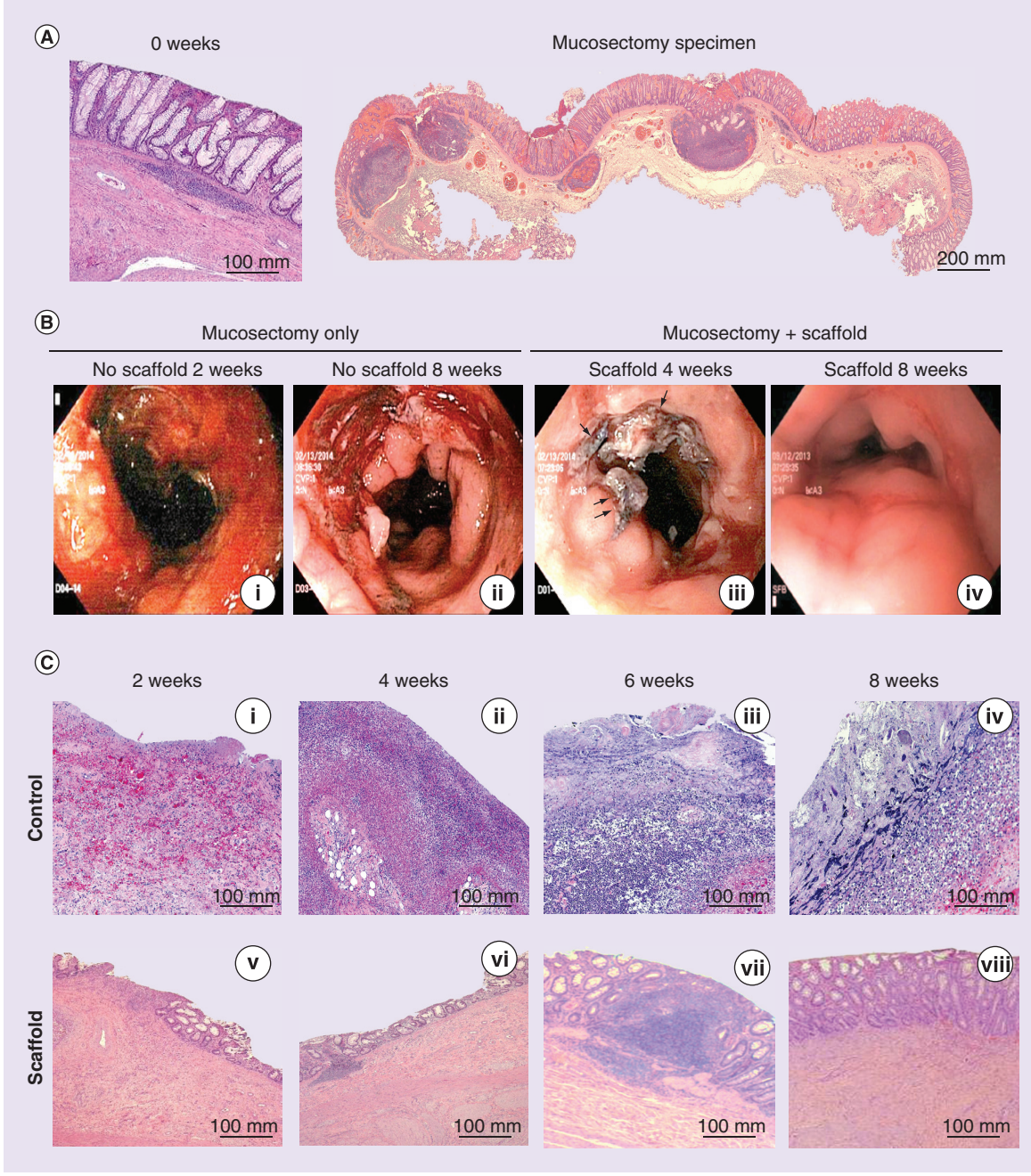

Figure 7. Evaluation of the ability of a novel tubularized 3D intestinal scaffold to support the growth of the colonic mucosa in a canine mucosectomy model. (Ai) Representative H&E micrograph of the mucosectomy specimen obtained from the rectum and distal colon of a dog; **Aii**: H&E image of the entire circumferential rectal mucosectomy resection. **(B)** Representative video images obtained at colonoscopy in dogs that had been subjected to mucosectormy of the rectum and distal colon either without **(i–ii)** or with the implantation of the scaffold **(iii–iv)** at 2, 4 and 8 weeks after surgery as indicated. Arrows reveal sutures at the anastomosis site. **(C)** Representative H&E images of the mucosectomy site in dogs in the absence **(i–iv)** or presence **(v–viii)** of the implanted scaffold at 2 **(i, v)**, 4 **(ii, vi)**, 6 **(iii, vii)** and 8 **(iv, viii)** weeks.

Future perspective

Until recently, the field of tissue engineering has been largely focused on understanding the characteristics of individual progenitor cells (i.e., stem cells), and the various interactions between these cells and the underlying matrix on which their growth and differentiation is supported. Now that progenitor cells can be grown and genetically manipulated in a fairly straight forward manner, the field of tissue engineering is poised to enter an entirely new phase, one in which the interactions

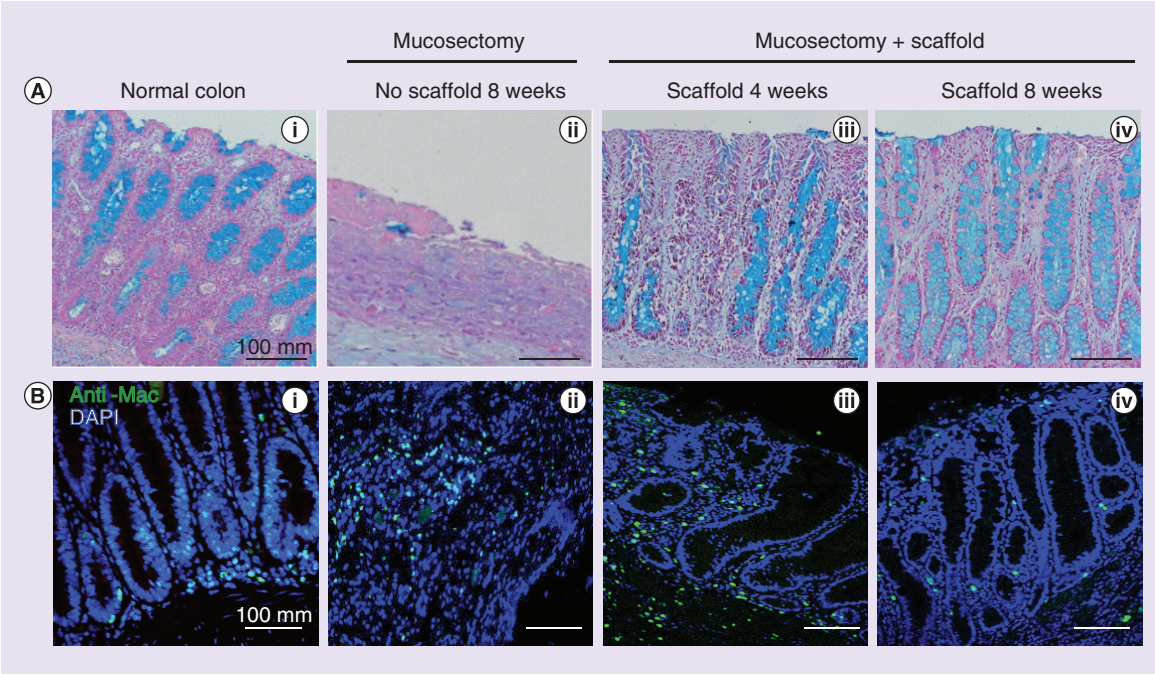

Figure 8. Evaluation of the ability of a novel 3D intestinal scaffold to support regeneration of colon in a canine mucosectomy model. (A) Representative micrographs of tissue sections obtained at the mucosectomy site that had been stained for the goblet cell marker Alcian Blue, in the absence of surgery **(i)**, 8 weeks after mucosectomy without scaffold **(ii)** or 4 **(iii)** or 8 weeks **(iv)** after mucosectomy with implantation of the scaffold. **(B)** Immunohistochemical evaluation of the inflammatory macrophage response within the dog colonic mucosa in normal colon **(Bi)**, 8 weeks following mucosectomy without placement of a scaffold **(Bii)** and at 4 and 8 weeks following mucosectomy with placement of a scaffold **(Biii & iv)**.

between stem cells and other nonprogenitor cellular components that are found within intact tissue can be explored. These studies will also enhance our ability to understand how native and synthetic tissue can respond to various environmental and microbial pressures, and the effects of these pressures on stem cell function. It is possible that the precise modes of communication and the effects of different cell types on various biological matrices will be elucidated in some detail, such that the ability to design and synthesize functional organs for therapeutic purposes is likely to be significantly accelerated. It is hoped that the current study, and studies like it, may be viewed in this broader context of seeking to understand how various cell components interact in order to achieve the goal of designing a replacement organ that is fundamentally similar to its native counterpart.

Financial & competing interests disclosure

This work was funded by a Hartwell Biomedical Collaborative Research Award to DJ Hackam and JC March. DJ Hackam is supported by R01GM078238 and RO1DK08752. The authors have no other relevant affiliations or financial involvement with any organization or entity with a financial interest in or financial conflict with the subject matter or materials discussed in the manuscript apart from those disclosed.

No writing assistance was utilized in the production of this manuscript.

Ethical conduct of research

All mice experiments were approved by the Animal Care and Use Committee of the University of Pittsburgh. All human tissue was obtained with approval from the University of Pittsburgh Institutional Review Board and in accordance with the University of Pittsburgh anatomical tissue procurement guidelines. Tissue was obtained from discarded pathological specimens at the time of surgery and therefore informed consent was not obtained from patients as no undo harm was expected to the de-identified patients. The authors have followed the principles outlined in the Declaration of Helsinki for all human or animal experimental investigations. In addition, for investigations involving human subjects, informed consent has been obtained from the participants involved.

Supplementary data

To view the supplementary data that accompany this paper please visit the journal website at: http://www.futuremedicine.com/doi/full/10.2217/RME.15.70

Executive summary

The growth & differentiation of intestinal progenitor cells are modified by cellular & microbial elements of the native stem cell niche

- The growth and differentiation of intestinal progenitor cells into enteroids is enhanced in the presence of myofibroblasts and polarized M2 macrophages.
- The addition of the probiotic *lactobaccilus* leads to improved enteroid enterocyte proliferation and increased differentiation into paneth cells.
- The presence of bacteria from the stool of infants with severe gut inflammation adversely affects intestinal stem cell growth and differentiation.

A tubularized, absorbable bioscaffold with villi projections that resemble the native intestine promotes the growth & differentiation of intestinal progenitor cells

- The culture of intestinal progenitor cells with and without intestinal niche components can be successfully obtained on a novel tubular bioscaffold that bears resemblance to the native small intestine.

Intestinal progenitor cells derived from mouse & human ileum can generate donor-derived epithelial structures covering a tubular scaffold following murine omental implantation

- Using the murine omentum as a biological bioreactor, murine and human enteroids seeded on a novel 3D scaffold generate epithelial structures surrounding the villi of the scaffold.
- Immunohistochemistry shows an initial controlled inflammatory reaction which diminishes over time and is associated with a robust vascular in growth and increase in proremodeling pericyte stem cells.

Use of the 3D Scaffold in an intestinal mucosal defect without seeded cells is biocompatible & leads to neointestinal regeneration in a large animal model

- Implantation of a 3D polymer scaffold into a mucosal defect leads to mucosal regeneration with similar characteristics as the native colonic mucosa.

Conclusions

- An intestinal epithelium can be engineered to grow on a tubular scaffold with an architecture that resembles the native intestine including the presence of villous structures, when cultured in the presence of appropriate intestinal niche and microbial components, suggesting that a tissue-engineered small intestine may be developed for clinical use in patients with short bowel syndrome or intestinal failure.

References

Papers of special note have been highlighted as: • of interest; •• of considerable interest

1 Belchior GG, Sogayar MC, Grikscheit TC. Stem cells and biopharmaceuticals: vital roles in the growth of tissue-engineered small intestine. *Semin. Pediatr. Surg.* 23(3), 141–149 (2014).

2 Levin DE, Sala FG, Barthel ER *et al.* A "living bioreactor" for the production of tissue-engineered small intestine. *Methods Mol. Biol.* 1001, 299–309 (2013).

• **Methodology paper explaining the use of the murine omentum as a source for vital nutrients and vascularization for the growth of intestinal progenitor cells into small intestinal epithelium.**

3 Brugmann SA, Wells JM. Building additional complexity to *in vitro*-derived intestinal tissues. *Stem Cell Res. Ther.* 4(Suppl. 1), S1 (2013).

4 Spurrier RG, Speer AL, Grant CN, Levin DE, Grikscheit TC. Vitrification preserves murine and human donor cells for generation of tissue-engineered intestine. *J. Surg. Res.* 190(2), 399–406 (2014).

5 Grant CN, Grikscheit TC. Tissue engineering: a promising therapeutic approach to necrotizing enterocolitis. *Semin. Pediatr. Surg.* 22(2), 112–116 (2013).

6 Torashima Y, Levin DE, Barthel ER *et al.* Fgf10 overexpression enhances the formation of tissue-engineered small intestine. *J. Tissue Eng. Regen. Med.* doi:10.1002/term.1720 (2013) (Epub ahead of print).

7 Gupta A, Vara DS, Punshon G, Sales KM, Winslet MC, Seifalian AM. *In vitro* small intestinal epithelial cell growth on a nanocomposite polycaprolactone scaffold. *Biotechnol. Appl. Biochem.* 54(4), 221–229 (2009).

8 Lahar N, Lei NY, Wang J *et al.* Intestinal subepithelial myofibroblasts support *in vitro* and *in vivo* growth of human small intestinal epithelium. *PLoS ONE* 6(11), e26898 (2011).

• **Key original article describing the importance of intestinal myofibroblasts in coculture with enteroids serving as a vital niche component by providing important growth factors.**

9 Costello CM, Hongpeng J, Shaffiey S *et al.* Synthetic small intestinal scaffolds for improved studies of intestinal differentiation. *Biotechnol. Bioeng.* 111(6),1222–1232 (2014).

10 Lee J, Kaletunc G. Evaluation of the heat inactivation of Escherichia coli and *Lactobacillus plantarum* by differential scanning calorimetry. *Appl. Environ. Microbiol.* 68(11), 5379–5386 (2002).

11 Bondow BJ, Faber ML, Wojta KJ, Walker EM, Battle MA. E-cadherin is required for intestinal morphogenesis in the mouse. *Dev. Biol.* 371(1), 1–12 (2012).

12 Afrazi A, Branca MF, Sodhi CP *et al.* Toll-like receptor 4-mediated endoplasmic reticulum stress in intestinal crypts induces necrotizing enterocolitis. *J. Biol. Chem.* 289(14), 9584–9599 (2014).

13 Ying W, Cheruku PS, Bazer FW, Safe SH, Zhou B. Investigation of macrophage polarization using bone marrow

derived macrophages. *J. Vis. Exp.* (76), doi:10.3791/50323 (2013).

14 Costello CM, Sorna RM, Goh YL, Cengic I, Jain NK, March JC. 3D intestinal scaffolds for evaluating the therapeutic potential of probiotics. *Mol. Pharm.* 11(7), 2030–2039 (2014).

15 Good M, Sodhi CP, Ozolek JA *et al. Lactobacillus rhamnosus* HN001 decreases the severity of necrotizing enterocolitis in neonatal mice and preterm piglets: evidence in mice for a role of TLR9. *Am. J. Physiol. Gastrointest. Liver Physiol.* 306(11), G1021–G1032 (2014).

16 Nigro G, Rossi R, Commere PH, Jay P, Sansonetti PJ. The cytosolic bacterial peptidoglycan sensor Nod2 affords stem cell protection and links microbes to gut epithelial regeneration. *Cell Host Microbe* 15(6), 792–798 (2014).

17 Sato T, Vries RG, Snippert HJ *et al.* Single Lgr5 stem cells build crypt-villus structures *in vitro* without a mesenchymal niche. *Nature* 459(7244), 262–265 (2009).

•• **Groundbreaking original research describing the ability to culture isolated intestinal crypt cells in a mesenchymal-free culture to generate intestinal structures mimicking the native intestinal architecture.**

18 Barker N, Van Es JH, Kuipers J *et al.* Identification of stem cells in small intestine and colon by marker gene Lgr5. *Nature* 449 1003–1007 (2007).

•• **Original article describing the breakthrough finding of a rapidly cycling intestinal stem cell marker identified by the Wnt target gene *LGR5* through a series of elegant and novel experiments.**

19 Erlandsen SL, Parsons JA, Taylor TD. Ultrastructural immunocytochemical localization of lysozyme in the Paneth cells of man. *J. Histochem. Cytochem.* 22(6), 401–413 (1974).

20 Fre S, Huyghe M, Mourikis P, Robine S, Louvard D, Artavanis-Tsakonas S. Notch signals control the fate of immature progenitor cells in the intestine. *Nature* 435(7044), 964–968 (2005).

21 Winterford CM, Walsh MD, Leggett BA, Jass JR. Ultrastructural localization of epithelial mucin core proteins in colorectal tissues. *J. Histochem. Cytochem.* 47(8), 1063–1074 (1999).

22 Varndell IM, Lloyd RV, Wilson BS, Polak JM. Ultrastructural localization of chromogranin: a potential marker for the electron microscopical recognition of endocrine cell secretory granules. *Histochem. J.* 17(9), 981–992 (1985).

23 Ozerdem U, Grako KA, Dahlin-Huppe K, Monosov E, Stallcup WB. NG2 proteoglycan is expressed exclusively by mural cells during vascular morphogenesis. *Developmental Dynamics* 222(2), 218–227 (2001).

24 Russell KC, Tucker HA, Bunnell BA *et al.* Cell-surface expression of neuron-glial antigen 2 (NG2) and melanoma cell adhesion molecule (CD146) in heterogeneous cultures of marrow-derived mesenchymal stem cells. *Tissue Eng. A* 19(19–20), 2253–2266 (2013).

25 Grant CN, Mojica SG, Sala FG *et al.* Human and mouse tissue-engineered small intestine both demonstrate digestive and absorptive function. *Am. J. Physiol. Gastrointest. Liver Physiol.* 308(8), G664–G677 (2015).

26 Yu J, Peng S, Luo D, March JC. *In vitro* 3D human small intestinal villous model for drug permeability determination. *Biotechnol. Bioeng.* 109(9), 2173–2178 (2012).

• **The initial description of the novel 3D villous scaffold used in the current manuscript with assessment showing close similarities to absorptive profile of the native intestine.**

27 Clevers H, Loh KM, Nusse R. Stem cell signaling. An integral program for tissue renewal and regeneration: Wnt signaling and stem cell control. *Science* 346(6205), 1248012 (2014).

28 Cosin-Roger J, Ortiz-Masia D, Calatayud S *et al.* M2 macrophages activate WNT signaling pathway in epithelial cells: relevance in ulcerative colitis. *PLoS ONE* 8(10), e78128 (2013).

• **Original article describing the importance of M2 macrophages in the colon as drivers of Wnt signaling and LGR5 intestinal stem cells.**

29 Ciorba MA, Riehl TE, Rao MS *et al. Lactobacillus* probiotic protects intestinal epithelium from radiation injury in a TLR-2/cyclo-oxygenase-2-dependent manner. *Gut* 61(6), 829–838 (2012).

• **Original article evaluating the protective role of *Lactobacillus* from intestinal damage through the pattern recognition protein TLR2 and improves crypt survival.**

30 Sodhi CP, Shi XH, Richardson WM *et al.* Toll-like receptor–4 inhibits enterocyte proliferation via impaired beta-catenin signaling in necrotizing enterocolitis. *Gastroenterology* 138 185–196 (2010).

• **Original description of the role of bacterial receptor TLR4 in the regulation of gut mucosal homeostasis.**

31 Neal MD, Sodhi CP, Jia H *et al.* Toll-like receptor 4 is expressed on intestinal stem cells and regulates their proliferation and apoptosis via the p53 up-regulated modulator of apoptosis. *J. Biol. Chem.* 287(44), 37296–37308 (2012).

32 Sodhi CP, Neal MD, Siggers R *et al.* Intestinal epithelial Toll-like receptor 4 regulates goblet cell development and is required for necrotizing enterocolitis in mice. *Gastroenterology* 143(3), 708–718 e701–705 (2012).

33 Brower-Sinning R, Zhong D, Good M *et al.* Mucosa-associated bacterial diversity in necrotizing enterocolitis. *PLoS ONE* 9(9), e105046 (2014).

34 Lelouard H, Fallet M, De Bovis B, Meresse S, Gorvel JP. Peyer's patch dendritic cells sample antigens by extending dendrites through M cell-specific transcellular pores. *Gastroenterology* 142(3), 592–601 e593 (2012).

35 Chieppa M, Rescigno M, Huang AY, Germain RN. Dynamic imaging of dendritic cell extension into the small bowel lumen in response to epithelial cell TLR engagement. *J. Exp. Med.* 203(13), 2841–2852 (2006).